Distinguishing and phenotype monitoring of traumatic brain injury and post-concussion syndrome including chronic migraine in serum of Iraq and Afghanistan war veterans

Jay S. Hanas[1,2,3]*, **James R. S. Hocker**[1], **Megan R. Lerner**[2], **James R. Couch**[4,5]

1 Department of Biochemistry, University of Oklahoma College of Medicine, Oklahoma City, Oklahoma, United States of America, **2** Department of Surgery, University of Oklahoma College of Medicine, Oklahoma City, Oklahoma, United States of America, **3** Veterans Administration Hospital, Oklahoma City, Oklahoma, United States of America, **4** Department of Neurology, University of Oklahoma College of Medicine, Oklahoma City, Oklahoma, United States of America, **5** Department of Neurology, Veterans Administration Hospital, Oklahoma City, Oklahoma, United States of America

* jay-hanas@ouhsc.edu

Abstract

Traumatic Brain Injury (TBI) and persistent post-concussion syndrome (PCS) including chronic migraine (CM) are major health issues for civilians and the military. It is important to understand underlying biochemical mechanisms of these conditions, and be able to monitor them in an accurate and minimally invasive manner. This study describes the initial use of a novel serum analytical platform to help distinguish TBI patients, including those with post-traumatic headache (PTH), and to help identify phenotypes at play in these disorders. The hypothesis is that physiological responses to disease states like TBI and PTH and related bodily stresses are reflected in biomolecules in the blood in disease-specific manner. Leave one out (serum sample) cross validations (LOOCV) and sample randomizations were utilized to distinguished serum samples from the following TBI patient groups: TBI +PTSD + CM + severe depression (TBI "most affected" group) vs healthy controls, TBI "most affected" vs TBI, TBI vs controls, TBI + CM vs controls, and TBI + CM vs TBI. Inter-group discriminatory p values were $\leq 10^{-10}$, and sample group randomizations resulted in p non-significant values. Peptide/protein identifications of discriminatory mass peaks from the TBI "most affected" vs controls and from the TBI plus vs TBI minus CM groups yielded information of the cellular/molecular effects of these disorders (immune responses, amyloidosis/Alzheimer's disease/dementia, neuronal development). More specific biochemical disease effects appear to involve blood brain barrier, depression, migraine headache, autoimmunity, and autophagy pathways. This study demonstrated the ability for the first time of a novel, accurate, biomarker platform to monitor these conditions in serum, and help identify biochemical relationships leading to better understanding of these disorders and to potential therapeutic approaches.

Introduction

Traumatic brain injury (TBI) is a major health issue for civilians and for the military. Approximately 1.7 million TBIs are reported annually in the United States, with 275,000 hospitalizations, and 53,000 deaths [1]. A significant number of TBIs likely go unreported. TBI is problematic for the military with 15–20% of Soldiers deployed to Afghanistan and/or Iraq wars experiencing a deployment-related TBI (D-TBI) [2, 3]. A majority of TBIs, including in the military, are mild with loss of consciousness (LOC) <30 minutes [1–4]. TBI is often associated with the post-concussion syndrome (PCS) which can include chronic daily headache (CDH), post-traumatic stress disorder (PTSD), and/or depression, all of which are health concerns for both military personnel and civilians [5–7]. These PCS conditions can occur for extended periods of time after the D-TBI [1–4, 7–9]. Headache (HA) is the most frequent PCS symptom (referred to as post-traumatic headache-PTH), and is a problem that can persist/reoccur for months to years after the TBI [8–12]. Studies of veterans at 2–11 years after D-TBI, 98% reported continuing HA of which 45% had CDH (occurring $\geq$ 15 days/month); two thirds of these had chronic migraine (CM) [headache occurring $\geq$ 15 days/month with $\geq$ 8 of these being migraine]) [4, 13]. The prevalence of CM in deployed veteran controls (8%) was about four times the reported prevalence of CM in the civilian population of 1–2% [14, 15]. In these analyses 2–11 years after D-TBI, PTSD was found in about 60% of TBI patients and about 10% of controls [4]. Severe depression (SDep) was noted in 43% of the D-TBI patients and only in 6% of controls. D-TBI subjects with a combination of PTSD and/or severe depression was found in approximately 60% of those with CM. In patients with D-TBI and CM, the addition of PTSD and/or SDep make the headache severity worse and the diagnosis and treatment more complicated. These observations indicate in studies of TBI and PTH (including CM), especially associated with deployed veterans, consideration should be given to these related factors (PTSD and/or SDep) in an effort to better understand TBI PCS patient symptoms and their persistence and potential biochemical/physiological inter-relationships.

It is important to develop accurate molecular aids useful for monitoring these conditions, and for revealing mechanistic clues that could possibly aid in the development of therapies for individuals with these conditions, especially in their persistent state. Peripheral blood, plasma, and/or serum are ideal bodily fluids to learn detailed information about TBI and PCS disorders including PTH since minimally invasive procedures are used to procure this biomaterial in a quick, efficient and accurate manner. Molecular information gleaned from such material is hypothesized to be able to help classify these conditions, understand any underlying associations/biochemical mechanisms, and provide possible targets for future biomarkers and therapeutic interventions. A number of studies have provided evidence indicating the analysis of peripheral blood (e.g., serum, plasma, blood cells) holds promise as minimally invasive aid or tool to study and understand TBI and associated PCS sequelae. In a study of acute TBI followed up to 90 days post-TBI using plasma immuno-analysis, increased levels of glial fibrillary protein, Tau, and Amyloid beta were observed in mild TBI patients versus healthy controls, providing evidence for physiological connections between TBI and Alzheimer's disease (AD) [16]. A plasma micro RNA (miRNA) study of acute TBI identified several specific miRNA molecules whose levels decreased over 30 days after the TBI [17]. PTSD was found to be associated with increased blood levels of cytokines and suggests neuro-inflammation may be a key component in developing/maintaining this disorder [18]. Higher levels of serum inflammatory marker, C-reactive protein, were associated with severe depression (SDep) suggesting an inflammatory component of SDep [19]. Several blood biomarkers were reported to be associated with migraine headaches including CM. The calcitonin gene-related peptide (CGRP) is one such serum marker reported for acute migraine and CM [20]. An inflammatory

connection to migraine has been alluded to with the observations that serum acute phase proteins pentraxin-3 and fibrinogen are found associated with migraine duration [21].

Currently there are no biomarkers in clinical use approved to assist in distinguishing and monitoring patients with TBI and related PCS symptoms including CM, PTSD, and/or SDep. Evidence indicates these potential post-concussion effects of TBI can be observed >30 years after initial brain concussion [4, 22]. Most molecular studies on TBI and PCS biomarkers are performed in the early acute phases of the disorders and have ignored long-term variations. The present study is unique in that TBI and PCS including CM are being studied in a 5–14 year window after the initial concussion event. In this regard, it is important to see if such conditions can be monitored in an extended time frame in an accurate, robust, and straight-forward manner. In addition, molecular analysis of such a prolonged window may yield possible mechanisms to help explain the persistence of these disease states over time. One unique aspect, of this study, is the patient recruitment strategy which seeks out a narrow source of patients (veterans deployed to Mideast war theaters) with a large swath (plus or minus a D-TBI) of symptoms but with no recruiting emphasis on PTH and PCS. This created two pools of subjects from which subgroups based on occurrence of D-TBI, severity of TBI, type of headache, and presence of PTSD and/or depression could be created. A third unique feature of this study Is the use, for the first time in the TBI and headache field, of a minimal serum electrospray ionization mass spectrometry (ESI-MS) platform as a potential tool to help monitor and understand TBI and PTH. This platform has had success in the cancer field being able to distinguish both early-stage lung cancer and pancreatic cancer as well as provide mechanistic information about the diseases [23, 24]. The large number of different identifiers (serum mass peaks) used by this methodology, which differs from a number of other biomarker platforms which use far fewer identifiers, appear to provide the highly specific disease discrimination and elucidation ability of this platform. It is anticipated that this unique property of this platform will be successful in this present study [23, 25, 26].

Materials and methods

Patients and clinical samples

All study subjects were recruited from a listing of Operation Enduring Freedom (OEF) and Operation Iraqi Freedom (OIF) veterans in the Oklahoma City Veterans Administration Medical Center (VAMC) catchment area. This list was constructed from the VA Veterans Integrated Service Network (VISN-16 & VISN-19) Data Repository and contained 6,470 OEF/OIF veterans who had suffered a confirmed D-TBI and 16,345 possible control subjects who had not suffered a D-TBI (Fig 1). Of these totals, 4445 Subjects who lived within 100 miles of the Oklahoma City VA Medical Center or, if located farther away but received medical care at the OKC VAMC, were identified and contacted randomly to request their participation in the study. No other criteria were applied in selection for initial contact. The major inclusion criteria for this study were: (a) deployment to a war zone, (b) absence of major organ disease or infectious/inflammatory disease at the time of the D-TBI and at the time of interview, and (c) occurrence of a D-TBI for the TBI subjects, and absence of a D-TBI for controls. 167 subjects were recruited into the study from the above VISN list. Participants provided written consent (at the time of the blood draw) via a signed consent document approved by the University of Oklahoma Health Sciences Center Institutional Review Board of Human Subjects Research (IRB # 6839). During the scheduled appointment the individuals were interviewed, completed the required questionnaires (described in the next section and in S1 Appendix), and provided a peripheral blood sample from an arm vein. These study volunteers resulted from 319 scheduled appointments of individuals who fulfilled all the requirements of the study and who
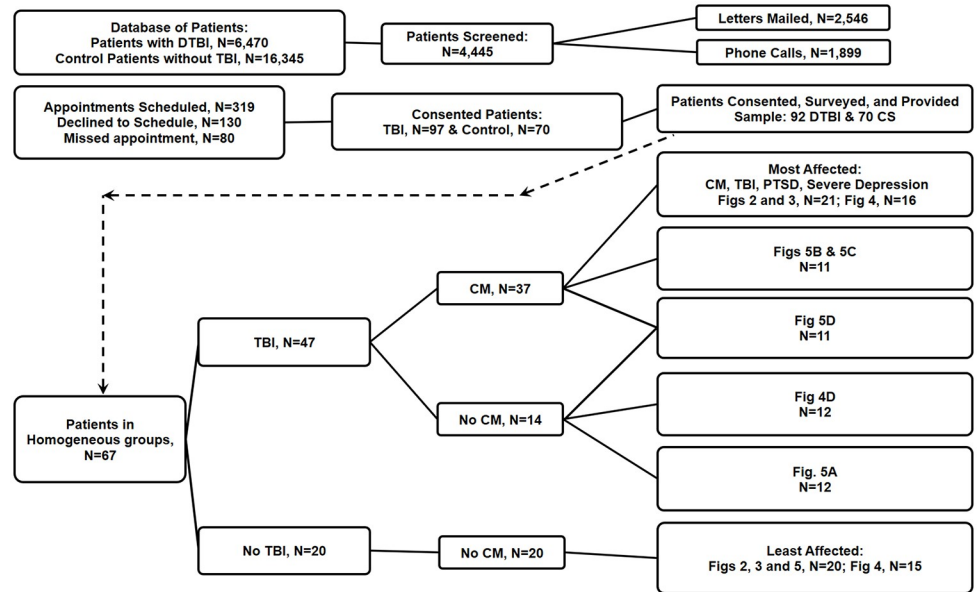
Fig 1. Study volunteer numbers, health characteristics, groupings, and figure inclusions. The number of patients available for recruitment, number of patients recruited, number of patients utilized, and the identification of the figures where these patients were utilized, are indicated.

https://doi.org/10.1371/journal.pone.0215762.g001

responded to our initial contacts (mailings or phone calls). Not all individuals scheduling appoints appeared for the consenting, interview, questionnaire, and blood draw process. 162 volunteers completed this entire process. Six of the 162 patients were females, and two were included in the present analysis of 65 volunteers, analysis method outlined in Fig 2, and with one female in Figs 3 and 4, and a different female in Fig 5. The remaining study subjects were males. The study breaks down with 47 subjects in the D-TBI group and 20 subjects in the
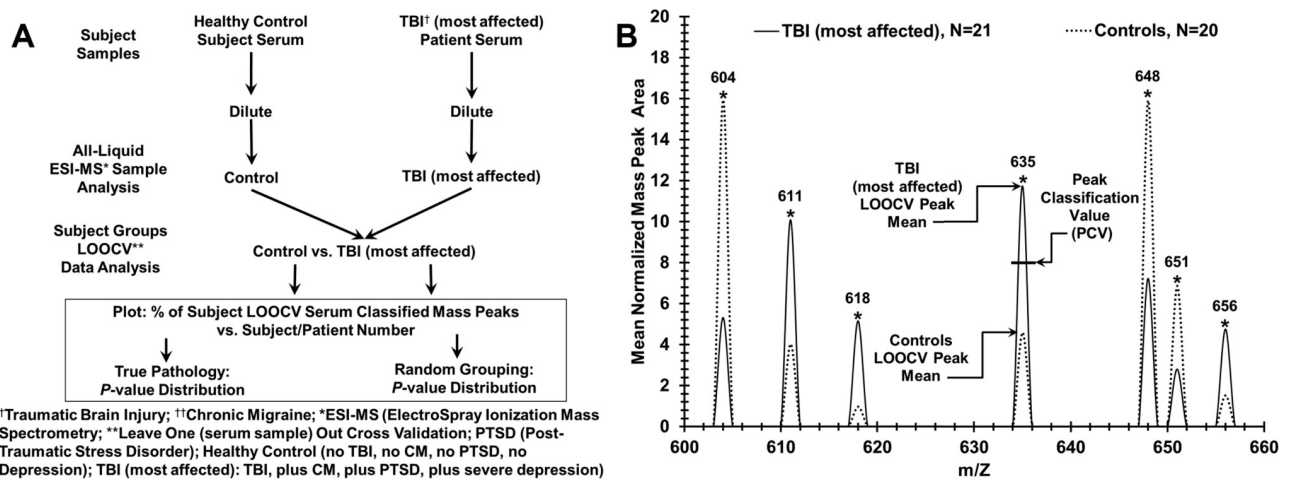
Fig 2. Experimental approach for discriminating sera from control individuals and patients with TBI and post- concussion syndrome (PCS) sequelae. (A) Flow chart for serum sample handling and mass spectrometry for binary patient/subject group analysis. Distinguishing control samples from TBI "most affected" samples is exhibited. (B) Peak Scoring for LOOCV (leave [one serum sample] out cross validation) procedure to classify mass peaks either "most affect" or control from a "left out" sample, over a narrow range (600–660 m/Z is displayed) of significant group discriminatory mass peaks. The PCV (peak classification value) example is exhibited on peak 635 which is used to classify "left out" peaks as either most affected (peak area above this PCV) or control (peak area at or below this PCV).

https://doi.org/10.1371/journal.pone.0215762.g002

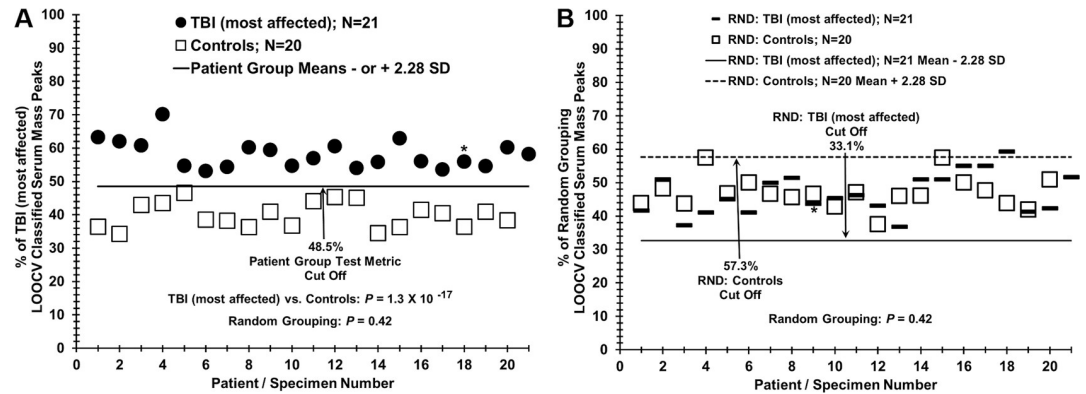**Fig 3. Distinguishing sera from TBI "most affected" patients versus controls using LOOCV and sample randomization analyses.** Male veterans of the United States Iraq and Afghanistan Wars were age-matched selected for these two different groups with similar war theater experiences but either having mild TBI and post-concussion sequelae PTSD and CM and SDep (most affected group) or lack of all these maladies (control group). (A) Serum discrimination of TBI most affected patients (dark circles) from controls (squares) by % of LOOCV classified mass peaks. A cut off value is present (- or + SDs from the most affected or control groups respectively) to determine test metric values (e.g. true positives). (B) Non-serum sample discrimination when the two different sample groups are mixed together randomly followed by the same LOOCV mass peak analysis. An * indicates a female volunteer and no experimental segregation is observed from the male volunteers in this analysis.

control, non D-TBI group. The final N values for the experiments and respective figures depicted in this study are also given in Fig 1. D-TBI subjects were recruited from veterans seen and diagnosed in the Oklahoma City VAMC (Veterans Administration Medical Center) TBI clinic. All TBI subjects had suffered their D-TBIs between 5 and 14 years prior to entering this study. The Volunteers consented to participate in the study and their blood samples were collected between January 1, 2017 to December 31, 2017.

Specific and pertinent patient/subject characteristics (e.g., PTSD and depression presence) for the 65 veteran serum samples used in the group comparison figures are given in Table 1.

Patients are partitioned with respect to sera presence in the respective figures (far left column). Individuals and their sera in figure column were deemed appropriate on the basis of having the most homogeneity for the following sample groupings: a) patients with TBI plus PTSD plus SDep plus CM (most affected), b) healthy control individuals (least affected: no TBI, no PTSD, no SDep, no CM), c) TBI alone (with minimal/no PTSD, SDep, CM contributions), d) TBI plus CM (with minimal/no PTSD, SDep, CM contributions). The 20 healthy controls used in this study out of the total of 70 were selected for best age-matching to the TBI "most affected" patients. All TBI subjects and control subjects were administered the same questionnaires (QS) which included: (1) TBI QS, (2) headache QS, (3) PTSD (civilian) QS, and (4) Beck Depression Inventory 2 (BDI 2). TBI was graded by duration of loss of consciousness (LOC) as mild—LOC of 1–30 minutes; moderate—LOC 30–360 minutes, and severe—LOC >6 hours. The majority of the D-TBI subjects in this study were graded "mild". Headache type was classified by criteria of International Classification of Headache disorders as migraine, tension, cluster, probable migraine or no headache [13]. PTSD *civ* score ranges assessed were ≤ 35, none, 36–49, possible PTSD, ≥ 50, highly probable PTSD. BDI 2 score ranges were ≤ 11, none, 12–19, mild depression, 20–28, moderate depression, ≥ 29, severe depression (SDep). Additional comprehensive patient characteristics are provided in S1–S6 Tables. Peripheral blood was obtained from consented control subjects or D-TBI patients in identical fashion at the Veterans Administration (VA) Hospital in Oklahoma City before any treatments. Blood (5 cc) was collected in no additive non-separator red stopper vacutainer
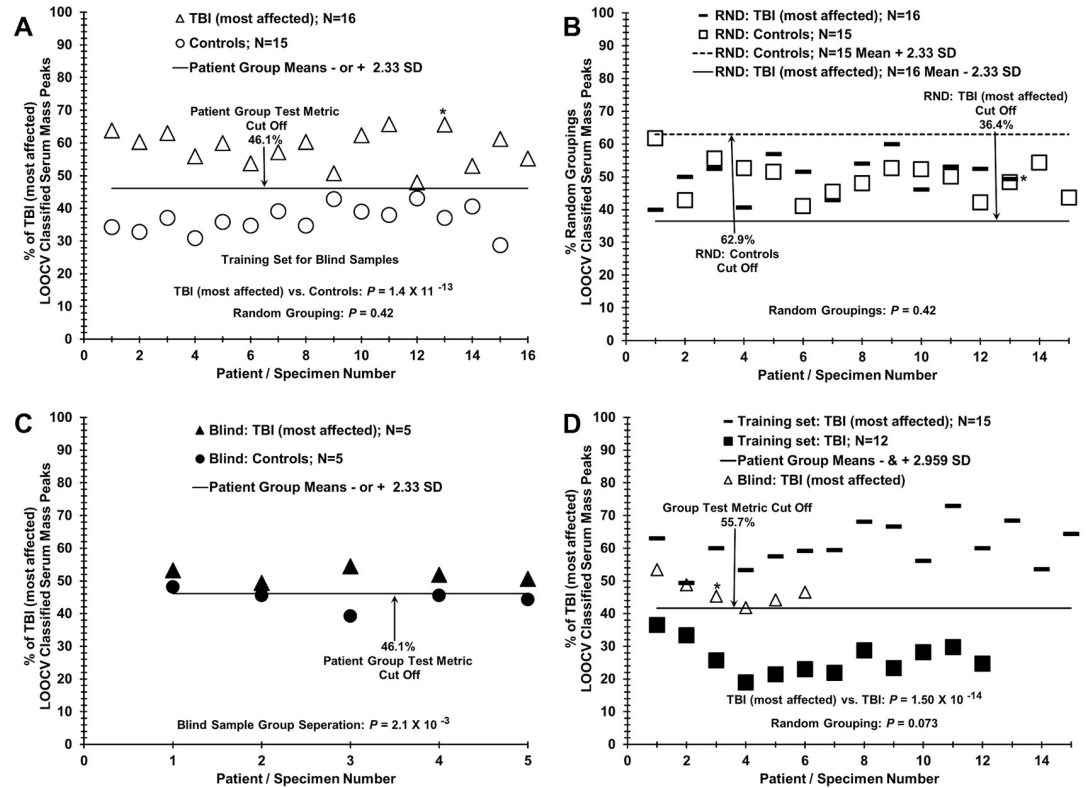
Fig 4. Analysis of blinded sera samples: Comparing patients with TBI+PCS versus controls or TBI alone. (A)Training set of serum discrimination of TBI most affected patients (triangles) from controls (circles) by % of LOOCV classified mass peaks; correct true positives and true negatives are observed. (B) Non-serum sample discrimination observed when the two different sample groups in panel A are mixed together randomly followed by the same LOOCV mass peak analysis. (C) Assessing the ability of the training set in panel A to correctly discriminate a blinded group of ten samples; 9 out of 10 samples were correctly identified. (D) Discrimination of sera from TBI most affected patients (dashes) from patients with TBI alone (dark squares), and assessment of 6 "left out" group of TBI most affected patients (triangles); 5 out of 6 blinded most affect patients were identified. An * indicates a female volunteer and no experimental segregation is observed from the male volunteers in this analysis.

tubes. Samples were allowed to clot at room temperature for 30 to 60 minutes and then spun at 4 ˚C for 10 minutes at 2,500 rpm. Serum aliquots of 250 µl were stored at -80 ˚C and thawed only once [27]. Patient protocols were reviewed and approved (# 6839) by a Human Subjects Institutional Review Board (IRB), at the University of Oklahoma Health Sciences Center and the Oklahoma City VA Hospital.

Electrospray mass spectrometry of sera from TBI and PCS veteran patients and from control veterans. A serum sample (4 µl) was diluted 1 to 300 into a solution of 50% methanol and 2% formic acid and separated into 3 aliquots. Triplicate mass spectra (20 minute averages) were collected from each TBI patient or control individual sera in random fashion. Spectra were sampled at a m/Z (mass divided by charge) resolution of two hundredths over a m/Z range of 400 to 2000 as previously described [24, 28] and in S2 Appendix. For tandem MS/MS structural analysis, ten serum samples from each patient/control group (TBI "most affected", control, and TBI plus CM, TBI minus CM) were selected randomly and analyzed in the ion-trap MS instrument as described previously [23, 24] and in S2 Appendix. Peak peptide/protein identifications were determined as described previously [23,24] and in S2 Appendix. Identified sequences were also searched using Basic Local Alignment Search Tool (BLAST) against NCBI human non-redundant database. Sequences were also compared against a *Taenia solium*
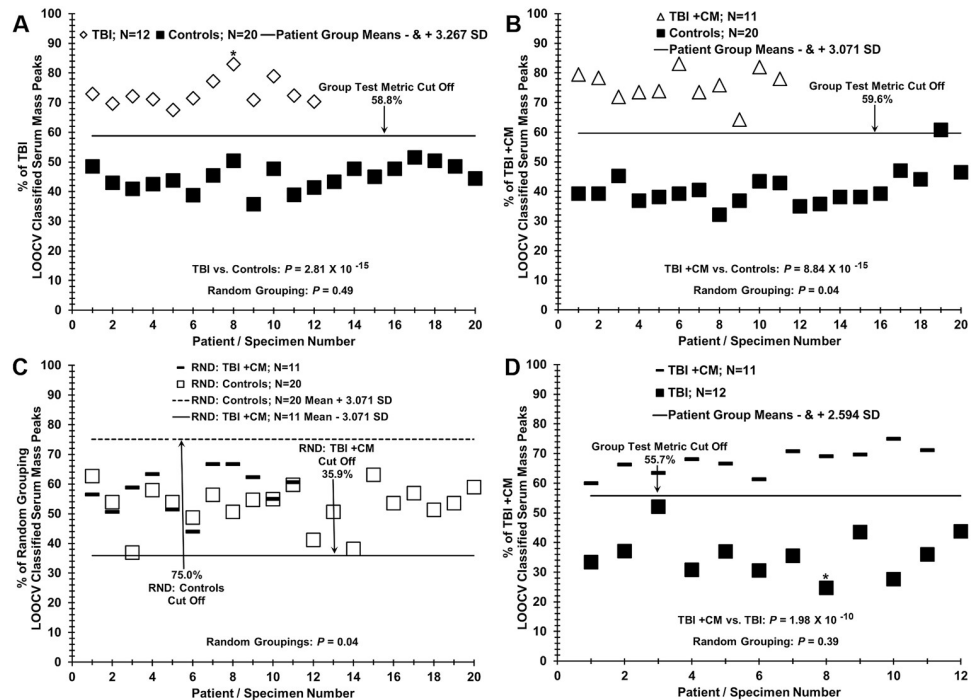
Fig 5. Distinguishing sera of TBI patients with and without chronic migraine (CM). (A) Sera discrimination of patients with TBI alone (diamonds) versus sera from control individuals (dark squares) by % of LOOCV classified mass peak analysis. (B) Sera discrimination of patients with TBI plus CM (triangles) versus sera from control individuals (dark squares). (C) Non-serum sample discrimination observed when the two different sample groups in B are mixed together randomly followed by the same LOOCV mass peak analysis. (D) Sera discrimination of patients with TBI plus CM (dashes) versus TBI alone (dark squares) by % of LOOCV classified mass peak analysis. An * indicates a female volunteer and no experimental segregation is observed from the male volunteers in this analysis.

https://doi.org/10.1371/journal.pone.0215762.g005

database to help rule out non-specific identifications. For Ingenuity Pathway Analysis (IPA, QIAGEN Redwood City, "www.qiagen.com/ingenuity"), identified gene/protein names, when present in 3 or more sera samples out of 10, and their corresponding numbers of Identified MS/MS peptide sequence "hits", were imported as log2 ratios for the control versus most affected TBI disorder comparison following similar work [23] and S3 Appendix. Proteins were also manually inspected for protein function and disease relatedness using PubMed/Medline. For IPA exhibited in Figs 6 and 7 in the main text, a neurological/immunological overview was incorporated into the IPA parameters used for those analyses. For IPA S1 and S2 Figs and in S3 Appendix, a TBI overview alone was incorporated for those figures. MS acquisition files are provided in S1–S17 Data. MS/MS acquisition files are provided in S18 Data.

Statistical and data processing/analysis

Data analyses are described here and in more detail in S2 Appendix. Mass spectral data were exported into Microsoft Excel in a format providing rounded unit m/Z and intensity values, and normalized/scaled to the highest m/Z sum intensity value in segments of 10 m/Z from 400–2000. Leave one out [serum sample] cross validation (LOOCV, described previously, was used to distinguish mass peaks in serum samples between the various binary groups, for example to distinguish mass peaks between the "most affected" patient group vs the control individual group ("least affected) [24]. LOOCV is employed to help mitigate "over-fitting" of large data sets [29, 30]. Mass peak area differences between the various binary group comparisons

Table 1. Patient characteristics.

Group characteristics and Figure identifier	Age in years	TBI (N)	PTSD (N):	Depression (N)	Headache (N)	Years since TBI
	Mean ±SD (range)	n, v-M, M, Mod	n, Poss, Prob	n/m, M, Mod, SDep	n, FH, CM	Mean ±SD (range)
All Patients						
All Patients, N = 65	43.29 ±8.38 (29–64)	20, 19, 21, 5	22, 9, 34	14, 27, 4, 20	33, 1, 31	10.89 ±2.48 (5–14)
All Controls, N = 20	44.05 ±8.8 (34–64)	20, 0, 0, 0	10, 0, 10	0, 20, 0, 0	20, 0, 0	na
All TBI, N = 45	42.96 ±8.26 (29–61)	0, 19, 21, 5	12, 9, 24	14, 7, 4, 20	13, 1, 31	10.89 ±2.48 (5–14)
Fig 3 panel A & Fig 3 panel B						
TBI (MA), N = 21	41.24 ±8.51 (29–61)	0, 7, 11, 3	6, 2, 13	0, 1, 0, 20	0, 1, 20	11.67 ±2.33 (6–14)
Controls, N = 20	44.05 ±8.8 (34–64)	20, 0, 0, 0	10, 0, 10	0, 20, 0, 0	20, 0, 0	na
RND: TBI (MA), N = 21	42.62 ±8.74 (30–64)	10, 5, 4, 2	8, 1, 12	0, 11, 0, 10	10, 1, 10	11.09 ±2.39 (6–14)
RND: Controls, N = 20	42.6 ±8.81 (29–61)	10, 2, 7, 1	8, 1, 11	0, 10, 0, 10	10, 0, 10	12.3 ±2.21 (7–14)
Fig 4 panel A & Fig 4 panel C						
TS TBI, (MA), N = 16	41.25 ±9.58 (29–61)	0, 7, 6, 3	4, 2, 10	0, 1, 0, 15	0, 1, 15	11.56 ±2.56 (6–14)
TS Controls, N = 15	43.87 ±10.23 (34–64)	15, 0, 0, 0	8, 0, 7	0, 15, 0, 0	15, 0, 0	na
TS RND: TBI (MA), N = 16	42.31 ±9.67 (29–64)	8, 1, 5, 2	6, 0, 10	0, 8, 0, 8	8, 0, 8	12.25 ±2.25 (7–14)
TS RND: Controls, N = 15	42.73 ±10.32 (30–61)	7, 6, 1, 1	6, 2, 7	0, 8, 0, 7	7, 1, 7	10.88 ±2.8 (6–14)
Blinds TBI (MA), N = 5	41.2 ±4.21 (37–47)	0, 0, 5, 0	2, 0, 3	0, 0, 0, 5	0, 0, 5	12 ±1.58 (10–14)
Blinds Control, N = 5	44.6 ±1.34 (43–46)	5, 0, 0, 0	2, 0, 3	0, 5, 0, 0	5, 0, 0	na
Fig 4 panel D						
TS TBI (MA), N = 15	43.73 ±8.15 (33–61)	0, 3, 10, 2	5, 1, 9	0, 0, 0, 15	0, 0, 15	12.33 ±1.54 (9–14)
TS TBI, N = 12	44.58 ±7.93 (30–57)	0, 7, 3, 2	3, 7, 2	7, 4, 1, 0	12, 0, 0	10.5 ±2.68 (5–14)
TS RND: TBI (MA), N = 15	44.07 ±7.1 (30–51)	0, 7, 5, 3	6, 3, 6	4, 2, 1, 0	7, 0, 8	10.87 ±2.47 (5–14)
TS RND: TBI, N = 12	44.17 ±9.15 (34–61)	0, 3, 8, 1	2, 5, 5	3, 2, 0, 7	5, 0, 7	12.33 ±1.78 (8–14)
Blinds TBI (MA), N = 6	35 ±6.16 (29–43)	0, 4, 1, 1	1, 1, 4	0, 1, 0, 5	0, 1, 5	10 ±3.22 (6–14)
Fig 5 panel A						
TBI, N = 12	45.25 ±6.85 (37–57)	0, 6, 4, 2	4, 7, 1	7, 4, 1, 0	12, 0, 0	11.17 ±2.12 (8–14)
Controls, N = 20	44.05 ±8.8 (34–64)	20, 0, 0, 0	10, 0, 10	0, 20, 0, 0	20, 0, 0	na
RND: TBI, N = 12	47 ±6.28 (37–57)	6, 3, 2, 1	8, 2, 2	3, 8, 1, 0	12, 0, 0	10.83 ±1.94 (8–13)
RND: Controls, N = 20	43 ±8.72 (34–64)	14, 3, 2, 1	6, 5, 9	4, 16, 0, 0	20, 0, 0	11.5 ±2.43 (8–14)
Fig 5 panel B & Fig 5 panel C						
TBI with CM, N = 11	44.91 ±8.37 (34–59)	0, 5, 6, 0	2, 0, 9	7, 2, 2, 0	0, 0, 11	9.64 ±2.16 (6–13)
Control, N = 20	44.05 ±8.8 (34–64)	20, 0, 0, 0	10, 0, 10	0, 20, 0, 0	20, 0, 0	na
RND: TBI with CM, N = 11	46.27 ±10.32 (34–64)	7, 1, 3, 0	3, 0, 8	3, 8, 0, 0	7, 0, 4	11.25 ±1.5 (10–13)
RND: Control, N = 20	43.3 ±7.44 (34–58)	13, 4, 3, 0	9, 0, 11	4, 14, 2, 0	13, 0, 7	8.71 ±1.98 (6–12)
Fig 5 panel D						
TBI with CM, N = 11	44.91 ±8.37 (34–59)	0, 5, 6, 0	2, 0, 9	7, 2, 2, 0	0, 0, 11	9.64 ±2.16 (6–13)
TBI, N = 12	45.25 ±6.85 (37–57)	0, 6, 4, 2	4, 7, 1	7, 4, 1, 3	12, 0, 0	11.17 ±2.12 (8–14)
RND: TBI with CM, N = 11	43.18 ±7.48 (34–56)	0, 5, 5, 1	0, 4, 7	6, 4, 1, 0	5, 0, 6	11.36 ±2.06 (8–14)
RND: TBI, N = 12	46.83 ±7.27 (36–59)	0, 6, 5, 1	6, 3, 3	8, 2, 2, 0	7, 0, 5	9.58 ±2.11 (6–13)

MA (most affected); TS (training set); SD (standard deviation); TBI (traumatic brain injury); PTSD (post-traumatic stress disorder); n (none); v-M (very mild); M (mild); Mod (moderate); Poss (possible); Prob (probable); n/m (none/minimal); SDep (severe depression); FH (frequent headache); CM (chronic migraine); na (not applicable)

used in the LOOCV analysis were identified as differing significantly at individual m/Z values using Student's t-tests (one-tailed, unequal variance, significance designated at $p < 0.05$, see Fig 2 panel B). A peak classification value (PCV) metric is assigned at the area midpoint between the two group means of each m/Z peak differing significantly in the "left in" binary
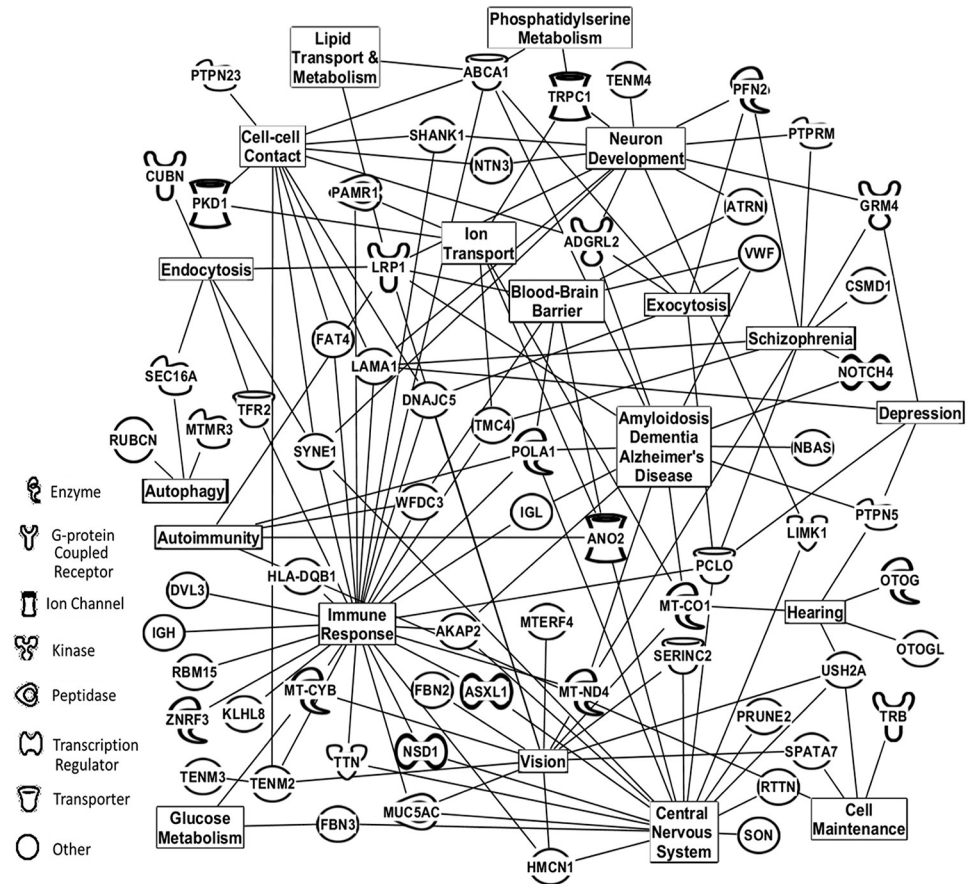
Fig 6. Physiological/cellular pathways of serum proteins found to distinguish TBI most affected patients from controls. Affected physiological/cellular pathways and serum protein assignments from Table 3 (top panel) that were found to distinguish TBI most affected patients from control individuals. The next top 58 proteins for each group (TBI most affected or control) not exhibited in Table 3 were added to the 48 in this table for this analysis. Analysis performed by using Ingenuity Pathway Analysis (IPA) bioinformatics software (Qiagen, Inc.).

https://doi.org/10.1371/journal.pone.0215762.g006

peak comparison dataset (e.g., peak 635, Fig 2 panel B). This midpoint is used to assign the group LOOCV classification for any "left out" peak in the LOOCV analysis. For example, if a "left out" samples identical m/Z peak has an area above this midpoint then that peak is classified as the larger peak area class. In the case of peak 635 this would be the most affected classification; if the area is equal to or below this value the peak classification would be "control". In this way a % of significantly changed mass peaks classified (e.g., as most affected) is assigned each "left out" sample and plotted on the y axis vs the individual serum samples on the x-axis (e.g., in Fig 3 panel A). Randomization of serum samples from subject groups compared in binary fashion (another method to assess data over-fitting) was obtained using the RAND function in Excel 2016 but retaining group number and age ratios [31]. Upon randomization, the identical mass peak LOOCV database was created and the same analysis described above was performed. To obtain potential statistical powers for group sample sizes (ability to detect type II errors-false negatives), Cohen's d effect size values are calculated from the binary group % LOOCV means and standard deviations in Table 2 [32, 33]. Statistical power using given sample sizes is calculated as described [33]. S1–S19 Tables provide spectral data, pre-averaged raw values and MS/MS data. Processing step result values are in S16, S17, S18 and S19 Tables.
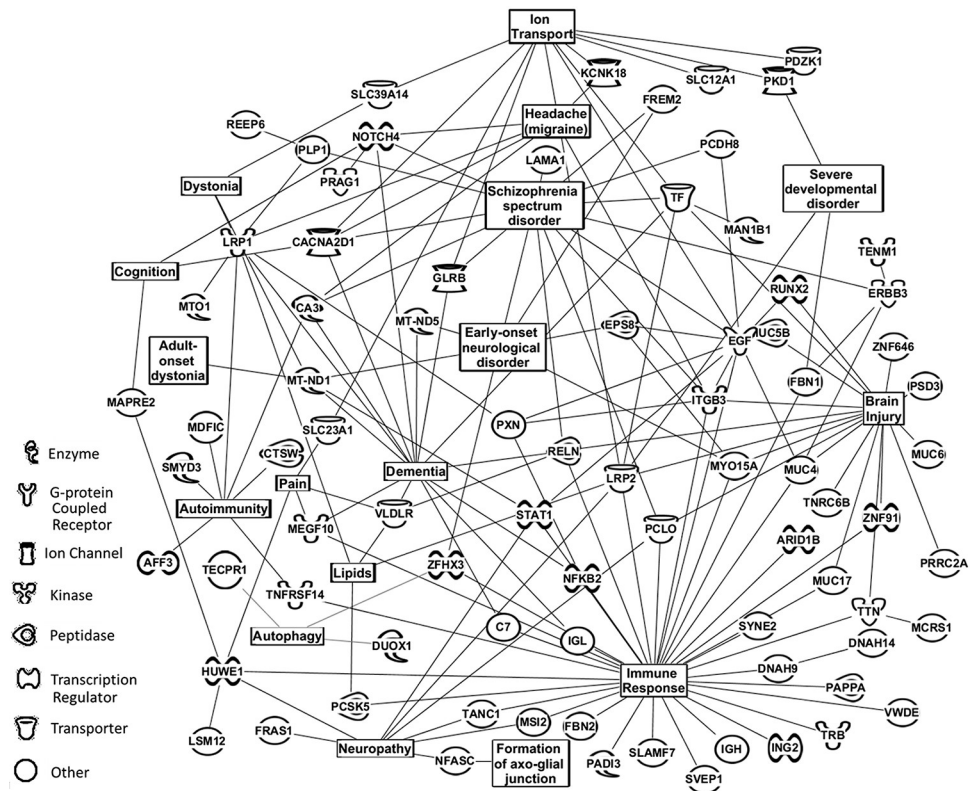
Fig 7. Physiological/cellular pathways of serum proteins found to distinguish TBI with CM from TBI only patients. Affected physiological/cellular pathways and serum protein assignments from Table 3 (bottom panel) that were found to distinguish patients with TBI alone versus patients with TBI plus CM. The next top 58 proteins for each group (TBI alone and TBI plus CM) not exhibited in Table 3 were added to the 48 in this table for this analysis. Analysis performed by using Ingenuity Pathway Analysis (IPA).

https://doi.org/10.1371/journal.pone.0215762.g007

Test metrics

The diagnostic value of a test/procedure is defined by its sensitivity, specificity, predictive value, and efficiency [34, 35]. Test sensitivity was determined from TP/(TP+FN) where TP was the number of true positives for disease presence, and FN was the number of false negatives for disease presence. Specificity was calculated from TN/(TN+FP) where TN is the number of true negatives and FP is the number of false positives. For example, TBI "most affected" and control TP, FP, TN, and FN values in Table 2 were determined using cutoffs of 2.28 standard deviations (SD) below the mean "% of TBI most affected LOOCV classified serum mass peaks, or 2.28 SD above the mean % control mass peaks (both cutoffs are represented by the single line in Fig 3 panel A).

Results

Using ESI-MS serum mass peak profiling to help distinguish "most affected" TBI patients from healthy control individuals

TBI in military veterans can occur in a clinical presentation involving other PCS sequelae including PTSD, SDep, and/or CM. It is important to study TBI and these sequelae together and individually to better understand these conditions and their interrelatedness and contributions to the overall clinical presentation. One goal of the present study is to examine whether

Table 2. LOOCV serum mass profiling test metrics.

Group 1 vs. Group 2	Mean (SD) Group 1	Mean (SD) Group 2	TP	TN	FP	FN	*P*-Value, Cohen's *d*	Random Grouping: *P*-Value	Figure #: panel
TBI (most affected), N = 21 vs. Controls, N = 20	58.16% (4.24%)	39.87% (3.80%)	21/21 (100%)	20/20 (100%)	0/20 (0%)	0/21 (0%)	1.3×10^{-17}, 4.54	0.42	3: A & B
Training Set A: TBI (most affected), N = 16 vs. Controls, N = 15	58.50% (5.33%)	39.87% (4.07%)	16/16 (100%)	15/15 (100%)	0/15 (0%)	0/16 (0%)	1.4×10^{-13}, 3.92	0.42	4: A & B
Blinded Set A: TBI (most affected), N = 16 vs. Controls, N = 15	51.90% (2.00%)	44.56% (3.28%)	5/5 (100%)	4/5 (80%)	1/5 (20%)	0/5 (0%)	2.1×10^{-3}, 2.70	na	4: C
Training Set B: TBI (most affected), N = 15 vs. TBI, N = 12	60.80% (6.49%)	26.28% (5.18%)	15/15 (100%)	12/12 (100%)	0/12 (0%)	0/15 (0%)	1.50×10^{-14}, 5.87	0.07	4: D
Blinded Samples B: (most affected), N = 6	46.71% (4.06%)	na	5/6 (83%)	na	na	1/6 (17%)	na	na	4: D
TBI; N = 12 vs. Controls, N = 20	73.13% (4.38%)	44.77% (4.31%)	12/12 (100%)	20/20 (100%)	0/20 (0%)	0/12 (0%)	2.81×10^{-15}, 6.52	0.49	5: A
TBI +CM; N = 11 vs. Controls, N = 20	75.81% (5.28%)	40.91% (6.09%)	11/11 (100%)	20/20 (100%)	0/20 (0%)	0/11 (0%)	8.84×10^{-15}, 6.12	0.04	5: B
TBI +CM; N = 11 vs. TBI; N = 12	67.41% (4.49%)	35.99% (7.62%)	11/11 (100%)	12/12 (100%)	0/12 (0%)	0/11 (0%)	1.98×10^{-10}, 5.02	0.39	5: C

Mean of the % Total LOOCV Sera Mass Peaks (Standard Deviation [SD]); True Positives (TP); True Negatives (TN); False Positives (FP); False Negatives (FN); Traumatic Brain Injury (TBI); Chronic Migraine (CM); Post Traumatic Stress Disorder (PTSD); not applicable (na); TBI Most Affected (TBI, plus CM, plus PTSD, plus severe depression); Controls (minus TBI, no CM, minus PTSD, minus Depression); TBI +CM (TBI, plus CM, minimal/no PTSD, minimal/no Depression); TBI (TBI, minimal/no PTSD, no CM, plus minimal/no depression)

the ESI-MS serum mass peak profiling methodology that has been successful in distinguishing early stage cancer patients from healthy controls as well as from different cancers, is able to distinguish TBI with PCS sequelae from healthy controls as well as distinguish TBI plus and minus PCS sequelae.

Fig 2 panel A is a flow chart outlining how serum mass peak profiling is employed to distinguish control individuals (least affected) from subjects with TBI, PTSD, SDep, and CM (most affected). The procedure requires a serum sample dilution (no pre-treatment or fractionation), and is a straight-forward biomolecule profiling platform. The complete mass peak database used here in Fig 2 (and also in Figs 3, 4 and 5, mean area values normalized) is provided in S6 Table. "Leave one out [serum sample] cross validation" (LOOCV) and group randomizations are employed to help mitigate and assess possible "over-fitting" of large data sets [29, 30]. Fig 2 panel B illustrates a small number of the significant ESI- MS mass peaks from 600 to 660 in m/Z units (mass divided by charge) able to discriminate sera from TBI "most affected" patients (solid line) from control individuals (dash line). This m/Z region is one of many analyzed (total range 400–2000 m/Z); the large number of significant peak differences likely is contributing to the disease discrimination ability of this technology [23, 25, 26]. These individual peak area means differ significantly (*p* value < 0.05) between 21 "most affected" patient sera samples and 20 control-"least affected" individual sera samples. Peak 635 exhibits a Peak Classification Value (PCV) metric area midpoint used for all peaks in the "left in" LOOCV database and is used to classify the group designations (either "most affected" or control-least affected) for the mass peaks in individual "left out" serum samples. A "left out" peak area above this midpoint is assigned to the higher value classifier ("most affected" for this peak, 635) and a "left out" peak equal to and below this midpoint is assigned to the lower value classifier (control for this peak). In this way individual "left out" serum samples are assigned a "% of total TBI most affected LOOCV classified mass peaks" or a "% of total control classified mass peaks" and that % value is plotted on the y-axis for each patient (x-axis, e.g., in Fig 3 panel A).

Fig 3 panel A illustrates the application of this LOOCV process for distinguishing patients with TBI "most affected" from healthy control individuals. When this "% of TBI most affected patient classified mass peaks value" (y axis) is plotted versus subject number (x-axis), a distribution plot is obtained (in which a clear demarcation is observed between most affected patients (darkened circles) versus controls (open squares). Individual LOOCV mass peaks identified and scored, on a per patient basis used in all the LOOCV binary group comparisons, are provided in S7–S10 Tables. The p value for this group discrimination is very low (10^{-17} range), and that value becomes non-significant (0.42) when these two different subject groups are mixed together in random fashion followed by the identical LOOCV mass peak analysis (Fig 3 panel B). This very large increase in p value upon inter-group sample randomization is consistent with minimal over-fitting of the original data set and with the presence of a physiological basis for the original TBI most affected versus control discriminations.

Distinguishing sera of TBI "most affected" patients from controls via blinded "test" sample analyses

A blinded validation experiment of the discriminatory power of ESI-MS in distinguishing sera from most affected TBI patients from that of healthy controls was performed by removing randomly 5 TBI most affected patient sera and 5 control individual sera (10 total) from each of the N = 21 and 20 subject groups. A "training set" was then assembled with N = 16 for the "most affected" and N = 15 for the control group ("most affected" vs control) with significant peaks selection using the LOOCV procedure. Fig 4 panel A exhibits the ESI-MS discrimination of the training set for these two groups based on % of TBI most affected patient sera LOOCV mass peaks (y axis) classified for each TBI and each control serum sample (x axis). For the training database, a very low discriminatory p value is obtained (10^{-13} range), and a p value of 0.42 (non-significance) is observed upon sample randomization of the known pathology group with the control group followed by the same LOOCV analysis. The p value 0.42 random "non-discrimination" is exhibited in panel B, and results of this "leave 10 serum samples out" blinded pathology" test validation in panel C. As can be observed, 9 out of the blind group of 10 "left out" serum samples were classified correctly with only one false positive for "most affected" (solid circle, above cut off value of 46.1% of "most affected" classified mass peaks). Another type of blinded analysis was performed by randomly removing 6 of the "most affected" samples and then test those samples against the same selected peak and area values from the training database constructed using the previously described LOOCV method on a "most affected" (N = 15) and TBI only (N = 12) patient set. Resulting data of the blinded sample testing are reported in Fig 4 panel D along with the training database patient scores ("most affected" in solid bars; TBI only solid squares) against the cutoff value of 55.7%. Five out of six samples were identified correctly (open triangles).

ESI-MS serum discrimination of patients with TBI plus or minus chronic migraine from each other and from control individuals

In order to examine the contribution of CM to the overall TBI clinical presentation, and conversely, to single out TBI and the CM phenotype from each other, the ability of ESI-MS serum mass profiling to discriminate these groups as well as controls was assessed. Exhibited in Fig 5 are binary ESI-MS LOOCV comparisons between serum samples from 20 control individuals, 12 TBI patients with no CM, and 11 TBI patients plus CM. Panel A of Fig 5 depicts ESI-MS distinguishing the TBI no CM patient serum sample set from the control serum set. A very low "true pathology" discrimination is obtained (p-value 10^{-15}) with a random grouping value of 0.49. Discriminating serum samples from patients with TBI plus CM from control individuals

is exhibited in panel B. One control false positive is observed (darkened square). The true pathology group discriminatory *p* value is very low (10^{-15}) but the random grouping value is slightly significant (0.04). Plotting this still significant group value in panel C indicates no real group discrimination is taking place (samples are indicated as true positives for the random (RND) TBI + CM group if above the solid line and also indicated as true negatives for the RND Control group if below the dashed line), as samples are identified as members of both random groups. Importantly, the ESI-MS profiling methodology is able to discriminate serum from TBI patients with CM (dashes) from TBI patients without CM (darkened squares, panel D). The true pathology *p* value is quite low (10^{-10}) and the random grouping value is non-significant (0.39).

Test metrics

Table 2 is a summary of the test metrics for the discriminatory mass peak data exhibited in Figs 3, 4 and 5. These metrics include the % LOOCV classified mass peak means and standard deviations (SD) for all the group comparisons (far left column) with respect to the specific figure panels (far right column). Nomenclature from predictive value theory is presented, e.g., test sensitivity, specificity, etc., as well as true pathology and random grouping *p* values [34, 35]. The pathological groups tested in binary fashion from these Figures are listed in the far-left column. The "% LOOCV MS peaks" means and their standard deviation (SD) are all well separated and have narrow SD boundaries for all the groups tested. Test sensitivities (true positive rate) range from 1.0 to 0.83 and test specificities (true negative rate) range from 1.0 to 0.80 for all groups. Physiological values in the original distribution differences are indicated by the very large increases in *p* values when the groups are randomized. A Cohen's *d* effect size value is provided in Table 2. "Effect size" refers to the mean differences for the binary group LOOCV discriminations observed in Figs 3, 4 and 5, taking into consideration the SD values [32]. This Cohen's *d* value is an indirect measure of statistical power (ability to detect type II errors-false negatives) of the sample sizes employed in a study. The large Cohen's *d* values exhibited here bolster the reliability and power (estimated from these effect sizes to be > 0.90) for the sample sizes used in this study (Table 2).

Serum peptide/protein identifications using MS/MS of LOOCV TBI "most affected", CM, and control group discriminatory mass peaks and bioinformatics cell pathway analysis

Table 3 exhibits MS/MS identified peptides listed by their protein name/abbreviations, their serum presence, and their numbers of MS/MS "hits" for the Fig 3 panel A TBI "most affected" versus control "least affected" binary LOOCV comparison (panel I, top 48 proteins) and for the Fig 5 panel D TBI plus and minus CM comparison (pane II, top 48 proteins). Individual selected LOOCV mass peaks identified and analyzed by MS/MS, on a per patient basis used in all the LOOCV binary group MS/MS comparisons, are provided in S11–S15 Tables. Notable serum peptide/protein changes (levels up or down in the two comparative groups) observed in panel I [shaded] with respect to post-traumatic neurological issues include GRM4 (glutamate receptor-4) and PCLO (protein Piccolo) which were previously suggested as biomarkers for major depression and possibly PTSD [36–38]. VWF (Von Willebrand Factor) was previously shown to have a role in maintaining blood brain barrier (BBB) flexibility, and ATRN has roles in myelination events which have been shown to be important in BBB protection and maintenance [39–41]. LRP1 is a major regulator of blood-brain barrier integrity [42]. Genetic evidence also indicates LRP1 is a susceptibility factor for migraine headache [43]. In addition, changes in LRP1 may have roles in dementia and Alzheimer's disease (AD) progression, as

Table 3. Peptides/proteins identified using LOOCV discriminatory mass peaks in TBI+PTSD+CM+SDep versus controls and TBI+CM versus TBI.

Least affected vs. Most affected (no. sera/10, no. MS/MS "hits"-least: no. MS/MS "hits" -most)

IGH (8, 9: 38)	SYNE1 (3, 57: 0)	TENM2 (3, 23: 11)	SIMC1 (3, 0: 15)
TTN (5, 54: 57)	FBN2 (3, 17: 32)	ATRN (3, 27: 0)	TNRC18 (3, 15: 0)
SSPO (4, 36: 44)	IGK (3, 21: 27)	PRUNE2 (3, 27: 0)	TCF20 (3, 13: 0)
NOTCH4 (4, 38: 36)	FAT4 (3, 13: 33)	FBN3 (3, 18: 8)	POLA1 (3, 8: 0)
IGL (4, 39: 26)	GRM4 (3, 0: 41)	ITGA8 (3, 0: 22)	DNAJC5 (2, 155:18)
PCLO (4, 4: 37)	LRP1 (3, 7: 33)	MALRD1 (3, 0: 19)	ADGRL2 (2, 171:0)
TRB (4, 15: 11)	MT-ND4 (3, 23: 16)	CSMD1 (3, 0: 17)	DNAJC5B (2, 6:151)
MUC19 (4, 0: 17)	HECTD4 (3, 23: 15)	PKD1 (3, 0: 16)	OTOGL (2, 38:90)
SON (3, 95: 0)	ZNRF3 (3, 36: 0)	C18orf15 (3, 15: 0)	EBF4 (2, 62:38)
LAMA5 (3, 39: 52)	NSD1 (3, 0: 35)	CNNM1 (3, 0: 15)	MUC2 (2,0:62)
MUC5AC (3, 24: 49)	USH2A (3, 19: 16)	PTPRM (3, 0: 15)	VWF (2, 13:45)
ZNF268 (3, 28: 34)	FCGBP (3, 22: 2)	SERINC2 (3, 0: 15)	TENM4 (2, 32:26)

TBI—CM vs TBI + CM (no. sera/10, no. MS/MS "hits"-CM: no. MS/MS "hits" + CM)

IGH (5, 31: 5)	MUC5B (3, 0:16)	PCLO (2, 0: 38)	DNAH9 (2, 20: 0)
MUC19 (4, 13: 12)	LSM12 (3, 9:0)	MAN1B1 (2, 36: 0)	IGFN1 (2, 6: 20)
EBF4 (3, 9: 107)	PCDH8 (3, 16: 0)	DKC1 (2, 32: 0)	ITGB3 (2, 19:0)
SYNE2 (3, 19: 75)	TRB (3, 14: 6)	SMYD3 (2, 21: 9)	SBF1 (2, 18: 0)
FBN2 (3, 76: 12)	RUNX2 (3, 13: 0)	RNF219 (2, 0: 28)	RELN (2, 0:18)
MT-ND5 (3, 12: 75)	MUC6 (3, 10: 0)	ARID1B (2, 28: 0)	PLOD1 (2, 0: 16)
IGL (3, 23: 46)	AFF3 (2, 200: 0)	FREM2 (2, 26: 0)	SLC12A1 (2, 16: 0)
TTN (3, 13: 41)	MT-ND1 (2, 20: 85)	CCDC18 (2, 24: 0)	DUOX1 (2, 0: 15)
HUWE1 (3, 33: 0)	PXN (2, 0: 45)	PADI3 (2, 24: 0)	TANC1 (2, 15: 0)
RXFP1 (3, 0: 21)	MAPRE2 (2, 42: 0)	ZKSCAN7 (2, 0: 23)	EGF (2, 5: 14)
TNRC6B (3, 34:14)	LAMA1 (2, 0:41)	ZNF571 (2, 0: 23)	LRP1 (2, 14: 4)
CCDC148 (3, 29:15)	ING2 (2, 40: 0)	PSD3 (2, 22: 0)	PLP1 (2, 0:14)

Shaded cells indicate neurological relationship

https://doi.org/10.1371/journal.pone.0215762.t003

does NOTCH4 [44, 45]. TBI has previously been shown to increase risks for dementia including AD in some cases 30 plus years after the initial injury [16, 25]. Of added interest, an autoimmunity pathway is present in Panel I with proteins LRP1 and POLA1 [46, 47]. Panel II exhibits the peptides/proteins identified by MS/MS whose serum levels are changing in TBI plus CM versus TBI minus CM patient comparison. A number of protein similarities are observed with Panel I including LRP1, a marker for migraine headache, and PCLO a possible marker for depression [37, 38, 43]. Also with respect to migraine is ITGB3 which was shown to influence serotonin blood levels, serotonin being previously implicated in migraine etiology [48, 49]. Dementia and AD potential markers are present in panel II, RXFP1, RELN, EGF and the previously mentioned LRP1 [50, 51]. TBI and dementia associations were previously demonstrated [16, 22]. HUWE1 mediated Notch signaling is involved in neuroprotection after injury [52]. Like in panel, I autoimmunity appears to be in play with proteins AFF3, SMYD3, and LRP1 [46, 53, 54]. Also of interest in panel II is autophagy with DUOX1, a protein involved in autophagic degradation pathways [55].

Fig 6 exhibits cellular/biochemical pathways that the bioinformatic software Ingenuity Pathway Analysis (IPA, QIAGEN Redwood City) indicated are being affected by including the list of 48 proteins in the TBI "most affected" versus "controls" exhibited in Table 3, panel I plus the next 58 ranked proteins not listed in that table. Neurological and immunological focuses were programmed into the IPA software pathway search for both Figs 6 and 7. Also included

in this pathway analysis as well as in Fig 7 are related functional inputs from literature searches on the 108 proteins described above using Medline and PubMed. Major pathways affected (by numbers of connections) in this TBI "most affected" versus control comparison include immune responses, central nervous system, neuron development/vision, and dementia/Alzheimer's disease. Also a depression pathway is identified involving aforementioned proteins GRM4, PCLO, plus protein PTPN5/STEP which has previously been associated with major depression and neuroinflammation [56]. As noted above a blood brain barrier phenotype is present as well as autoimmunity and autophagy with ANO2, HLA-DQB1, MTMR3, and SEC16A [57–60]. IPA analysis of the 48 proteins listed in panel II plus the next 58 ranked proteins for the TBI plus and minus CM comparison (Fig 5 panel D) is displayed in Fig 7. Major pathways identified as affected in this binary group comparison include immune responses, brain injury, dementia, and ion transport, similar to that observed in Fig 6. In addition, a migraine headache pathway of related proteins also appears in this comparison, most notably ITGB3, KCNK18, NOTCH4, and LRP1 which could be interacting with glutamate receptors [43, 48, 61–63]. Also the autoimmunity connections are present with AFF3, SMYD3, and LRP1 as well as autophagy with DUOX1, TECPR1, and ZHHX3 [64, 65]. It is noted that the IPA analysis illustrated in Figs 6 and 7 also include protein inputs from literature searches on disease relatedness of the proteins exhibited in Table 3 as well as the next top 58 proteins. IPA analysis including these proteins described above with a TBI focus is exhibited in S1 and S2 Figs. A TBI focus alone yields fewer pathway connections but possibly more direct information concerning the TBI condition. Additional IPA results and discussion and detail are provided in S4–S6 Appendices.

Discussion

Much research in the TBI and PCS field is focused on identifying short-term changes associated with TBI, while less attention has been paid to the long-term effects on patients. By observing individuals 5–14 years after the initial TBI, this present study focuses on the long-term physiological changes of PCS potentially induced by the TBI. By studying such long-term effects, it might be possible to obtain clues about mechanisms responsible for long-term persistence of PCS symptoms like chronic migraine headache. There are a number of unique aspects of this molecular and translational long-term study. The current experiments employ well-controlled subject group comparisons. The initial goal was to provide groups of D-TBI subjects who were recruited randomly from a listing, provided by the VA VISN 19 Data Repository, of approximately 6,000 Operation Enduring Freedom/Operation Iraqi Freedom (OEF/OIF) veterans who had suffered a confirmed D-TBI, and control veterans drawn from the same repository of approximately 12,000 OEF/OIF individuals who did not have a D-TBI. Thus, the non-TBI group of deployed veterans experienced the same war theater conditions as the veteran volunteers who suffered a deployment-related TBI. This also holds for the deployed veterans who did not manifest PCS associated PTSD, severe depression, and/or CM versus those deployed veterans who did. And as described above, these D-TBI veterans are in the persistent phases of their PCS disorders (5–14 years after their D-TBI) versus most previous studies on these disorders were in the earlier initial acute phase (less than 90 days). Therefore, veteran sera biomolecule analyses performed in this study should be able to provide additional clues concerning the underlying mechanisms for maintaining such persistence. Patient health and demographic data are provided in Table 1 in the main text and in S1–S3 Tables. The minimal serum mass profiling platform utilized in this study, employing leave one out (serum sample) cross validation [LOOCV] was able to uniquely discriminate groups of TBI and PCS sequelae patients from each other and from controls, as well as provide a set of discriminatory LOOCV

serum mass peaks whose identification should provide additional mechanistic clues about the biochemical nature of these disorders.

With respect to these patient groupings, it is important to develop such robust, accurate, and minimally invasive testing aids to assist researchers and clinicians in diagnosing, classifying, and monitoring individuals who sustained a TBI and developed PCS sequelae. Such aids will allow more vigilant screening of these conditions, helping with patient prognoses and treatments, and assist in the understanding of these disorders. This study reports progress in distinguishing individual serum samples from patients with D-TBI and post-concussion sequelae including PTSD, CM, and severe depression from each other and from control individuals, in retrospective and blinded fashion with high sensitivity and specificity test metrics (Table 2) 5–14 years after the initial TBI. In looking for possible independent variable effects on our LOOCV binary group comparisons, we assessed a number of such variables using R^2 variance analysis. We were not able to demonstrate a consistent R^2 association (observed range 0.0001 to 0.145) between the number of TBIs per patient and influence on the LOOCV binary comparison results. The one comparison with the higher R^2 value (0.749) was the blind analysis in Fig 4 panel C containing a small sample size which likely influenced the results. This information is provided in S4 Table. An R^2 analysis was performed showing no effect of age on any of the LOOCV binary comparisons in the study (observed range 0.0014 to 0.1998, S6 Table). Six of the 162 patients were females, and two were included in the present analysis of 65 volunteers in the Figures (one in Figs 3 and 4, and a different one in Fig 5). The remaining study subjects were males. The two female volunteers with TBI segregated with the male volunteers with TBI in the binary analyses. There were not enough females to make a direct male to female comparison. It was difficult to accumulate large N values for the matched groups in this study. However, the large "effect sizes" for these binary group comparisons (differences in mean mass peak areas/standard deviations for the two different groups in question which is proportional to statistical power-ability to detect false negatives) does lend credibility to the success of these discriminations even at the reduced sample sizes, and helps establish their validity and portends well for future studies with larger sample sizes [32]. Although the present study is a retrospective analysis, experiments were performed to begin to address the ability of this test procedure to discriminate blinded samples against a training set. In one blind test set (equal numbers of TBI "most affected" samples and controls) an analogous training set was able to correctly identify 9 out of 10 samples (Fig 4 panel C).

With respect to identifying underlying physiological process at play in these disorders, this ESI-MS platform also has the ability to "target" the unique binary group discriminatory set of LOOCV mass peaks for MS/MS structural determination which can lead to biochemical and phenotype elucidations. This represents a third and another unique aspect of this ESI-MS methodology: disease understanding through identification of a wide variety of biomolecules involved in disease mechanisms which can be performed with a very small sample of minimally-invasive bodily fluid. The identification of such biomolecules and biochemical pathways can aid in further biomarker and therapeutic development. Such analyses are presented in Table 3 and in Figs 6 and 7 for the TBI "most affected" versus controls and the TBI plus and minus CM comparisons, respectively. The biochemical/cellular pathway phenotypes identified playing a role in these disorders include inflammation/immune responses, neurological issues, and dementia/Alzheimer's disease inferences in Fig 6 and Fig. These observations are in line with previous evidences that TBI and associated post-concussion sequelae are triggering neuro-inflammation events, and the dementia/AD similarities observed in this study were noted before. Observing these known phenotypes lends credence to the ability of this serum profiling methodology and platform to help decipher these pathologies. These results indicate that we are separating/distinguishing these different groups based on actual physiological and pathological

differences which is consistent with the serum mass profiling hypothesis guiding these studies. Such disease differences reflected in the peripheral blood likely stem from systemic processes in response to such disease states as well as direct diseased tissue inputs [66, 67].

More novel and specific biochemical/cellular pathway affects observed in this study include a potential blood brain barrier (BBB) phenotype in the TBI "most affected" vs control and in the TBI plus and minus CM comparisons (Table 3, Figs 6 and 7). These observations about BBB effects in the present TBI study are in line with a previous analysis concerning effects of concussion on the BBB in humans and in rats [68]. Notably, a depression phenotype was observed in the TBI "most affected" vs control comparison (Table 3, Fig 6), and a migraine headache phenotype was observed in the TBI plus vs minus CM comparison (Table 3 and Fig 7). With respect to the persistence phenomenon associated with studies on the long-term pathologies of patients with TBI and associated PCS, the autoimmunity phenotype appearing in both the TBI "most affected" versus controls and the TBI plus versus minus CM IPA analyses (Figs 6 and 7) could provide a potential explanation for such persistence. Autoimmunity has recently been associated with stress-related disorders, and is known to have roles in other chronic diseases [69]. The long term persistence of TBI and associated PCS sequelae can be described as chronic diseases. Also the autophagy phenotype (cell degradation of intra-cellular constituents) is appearing in both Figs 6 and 7 IPA analyses, and autophagy was previously reported as a possible mechanism underlying TBI [70]. And of added interest, autophagy and autoimmunity are linked biochemically and physiologically [71]. This combination would be an ideal mechanism(s) to promote the persistence seen in long-term patients with TBI PCS related sequelae. By providing initial evidence of potential autoimmunity and autophagy mechanisms, this study provides basic observations which could open up new avenues of thought and future possible research concerning TBI and associated PCS sequelae including chronic migraine.

Supporting information

S1 Fig. IPA analysis of TBI "most affected" patients versus control subjects. Affected physiological/cellular pathways and serum protein assignments from Table 3 (main text) that were found to distinguish TBI most affected patients from control individuals. The next top 58 proteins for each group (TBI most affected or control) not exhibited in Table 3 were added to the 48 in this Table for this analysis. Analysis performed by using Ingenuity Pathway Analysis (IPA) bioinformatics software (Qiagen, Inc.) using a "TBI" focus in the software.
(TIF)

S2 Fig. IPA analysis of TBI plus CM patients versus TBI minus CM patients. Affected physiological/cellular pathways and serum protein assignments from Table 3 that were found to distinguish patients with TBI alone versus patients with TBI plus CM. The next top 58 proteins for each group (TBI alone and TBI plus CM) not exhibited in Table 3 were added to the 48 in this Table for this analysis. Analysis performed by using Ingenuity Pathway Analysis (IPA) using a "TBI" focus in the software.
(TIF)

S1 Appendix. Methods continued. TBI and PCS patient assessment and classification.
(DOCX)

S2 Appendix. Methods continued. Electrospray mass spectrometry of sera from patients with TBI and PCS and healthy controls.
(DOCX)

S3 Appendix. IPA figures and legends. S1 and S2 Figs. IPA analysis of TBI "most affected" patients versus control subjects with legends.
(DOCX)

S4 Appendix. IPA results continued. Cell pathways incorporating serum protein changes identified from MS/MS of LOOCV mass peaks discriminating TBI "most affected", CM, and control subject groupings using IPA software focus on "TBI".
(DOCX)

S5 Appendix. Discussion continued.
(DOCX)

S6 Appendix. Materials and methods continued. Patient characteristics.
(DOCX)

S1 Data. MS raw acquisition files ThermoFinnigan/ThermoFisher raw file format (1 of 17).
(ZIP)

S2 Data. MS raw acquisition files ThermoFinnigan/ThermoFisher raw file format (2 of 17).
(ZIP)

S3 Data. MS raw acquisition files ThermoFinnigan/ThermoFisher raw file format (3 of 17).
(ZIP)

S4 Data. MS raw acquisition files ThermoFinnigan/ThermoFisher raw file format (4 of 17).
(ZIP)

S5 Data. MS raw acquisition files ThermoFinnigan/ThermoFisher raw file format (5 of 17).
(ZIP)

S6 Data. MS raw acquisition files ThermoFinnigan/ThermoFisher raw file format (6 of 17).
(ZIP)

S7 Data. MS raw acquisition files ThermoFinnigan/ThermoFisher raw file format (7 of 17).
(ZIP)

S8 Data. MS raw acquisition files ThermoFinnigan/ThermoFisher raw file format (8 of 17).
(ZIP)

S9 Data. MS raw acquisition files ThermoFinnigan/ThermoFisher raw file format (9 of 17).
(ZIP)

S10 Data. MS raw acquisition files ThermoFinnigan/ThermoFisher raw file format (10 of 17).
(ZIP)

S11 Data. MS raw acquisition files ThermoFinnigan/ThermoFisher raw file format (11 of 17).
(ZIP)

S12 Data. MS raw acquisition files ThermoFinnigan/ThermoFisher raw file format (12 of 17).
(ZIP)

S13 Data. MS raw acquisition files ThermoFinnigan/ThermoFisher raw file format (13 of 17).
(ZIP)

S14 Data. MS raw acquisition files ThermoFinnigan/ThermoFisher raw file format (14 of 17).
(ZIP)

S15 Data. MS raw acquisition files ThermoFinnigan/ThermoFisher raw file format (15 of 17).
(ZIP)

S16 Data. MS raw acquisition files ThermoFinnigan/ThermoFisher raw file format (16 of 17).
(ZIP)

S17 Data. MS raw acquisition files ThermoFinnigan/ThermoFisher raw file format (17 of 17).
(ZIP)

S18 Data. MS/MS raw acquisition files ThermoFinnigan/ThermoFisher raw file format (1 of 1).
(ZIP)

S1 Table. Patient characteristics continued.
(DOCX)

S2 Table. Patient health history.
(DOCX)

S3 Table. Years since D-TBI.
(DOCX)

S4 Table. Relationship between D-TBI number and % LOOCV Patient scores.
(DOCX)

S5 Table. Volunteer specifications by pay grade.
(DOCX)

S6 Table. % Patient LOOCV score vs age.
(DOCX)

S7 Table. Normalized peak area mean for each patient by m/Z used for figures and tables.
(DOCX)

S8 Table. Patient % classified LOOCV mass peak scores plotted in presented figures.
(DOCX)

S9 Table. Samples used in each figure.
(DOCX)

S10 Table. Mass peaks selected by LOOCV process. MS peaks used by figure number.
(DOCX)

S11 Table. LOOCV MS/MS peaks utilized. Mass peaks selected for MS/MS analysis in Figs 6 and 7.
(DOCX)

S12 Table. Peptides identified using MS/MS by patient: TBI most affected vs control (least affected).
(DOCX)

S13 Table. Peptides identified using MS/MS by patient TBI + CM vs TBI.
(DOCX)

S14 Table. Proteins identified MSMS analysis TBI (most affected, N = 10) vs control (least affected, N = 10) MS/MS results.
(DOCX)

S15 Table. Proteins identified MSMS analysis TBI + CM (N = 10) vs TBI (N = 10) MS/MS results.
(DOCX)

S16 Table. Normalized peak data for averages.
(XLS)

S17 Table. Peaked data.
(XLS)

S18 Table. Normalized raw spectral data.
(XLS)

S19 Table. Raw spectral export.
(XLS)

Acknowledgments

Author Contributions

Conceptualization: Jay S. Hanas, James R. S. Hocker, Megan R. Lerner, James R. Couch.

Data curation: Jay S. Hanas, James R. S. Hocker, Megan R. Lerner, James R. Couch.

Formal analysis: Jay S. Hanas, James R. S. Hocker, James R. Couch.

Funding acquisition: Jay S. Hanas, James R. S. Hocker, James R. Couch.

Investigation: Jay S. Hanas, James R. S. Hocker, Megan R. Lerner, James R. Couch.

Methodology: Jay S. Hanas, James R. S. Hocker, Megan R. Lerner, James R. Couch.

Project administration: Jay S. Hanas, Megan R. Lerner, James R. Couch.

Resources: Jay S. Hanas, Megan R. Lerner, James R. Couch.

Software: Jay S. Hanas, James R. S. Hocker.

Supervision: Jay S. Hanas, James R. S. Hocker, Megan R. Lerner, James R. Couch.

Validation: Jay S. Hanas, James R. S. Hocker.

Visualization: Jay S. Hanas, James R. S. Hocker, James R. Couch.

Writing – original draft: Jay S. Hanas, James R. S. Hocker, Megan R. Lerner, James R. Couch.

Writing – review & editing: Jay S. Hanas, James R. S. Hocker, Megan R. Lerner, James R. Couch.

References

1. Theeler B, Lucas S, Riechers RG 2nd, Ruff RL. Post-traumatic headaches in civilians and military personnel: a comparative, clinical review. Headache. 2013 Jun; 53(6):881–900. https://doi.org/10.1111/head.12123 PMID: 23721236.

2. Hoge CW, Engel CC, Castro CA. Mild traumatic brain injury in US soldiers returning from Iraq—Reply. New Engl J Med. 2008 May 15; 358(20):2179-. English.

3. Theeler BJ, Flynn FG, Erickson JC. Headaches after concussion in US soldiers returning from Iraq or Afghanistan. Headache. 2010 Sep; 50(8):1262–72. https://doi.org/10.1111/j.1526-4610.2010.01700.x PMID: 20553333.

4. Couch JR, Stewart KE. Headache Prevalence at 4–11 Years After Deployment-Related Traumatic Brain Injury in Veterans of Iraq and Afghanistan Wars and Comparison to Controls: A Matched Case-Controlled Study. Headache. 2016 Jun; 56(6):1004–21. https://doi.org/10.1111/head.12837

5. Rao AS, Scher AI, Vieira RVA, Merikangas KR, Metti AL, Peterlin BL. The Impact of Post-Traumatic Stress Disorder on the Burden of Migraine: Results From the National Comorbidity Survey-Replication. Headache. 2015 Nov-Dec; 55(10):1323–41. English. https://doi.org/10.1111/head.12698 PMID: 26473981

6. Rist PM, Schurks M, Buring JE, Kurth T. Migraine, headache, and the risk of depression: Prospective cohort study. Cephalalgia. 2013 Sep; 33(12):1017–25. English. https://doi.org/10.1177/0333102413483930 PMID: 23588795

7. Lucas S, Smith BM, Temkin N, Bell KR, Dikmen S, Hoffman JM. Comorbidity of Headache and Depression After Mild Traumatic Brain Injury. Headache. 2016 Feb; 56(2):323–30. https://doi.org/10.1111/head.12762 PMID: 26814846.

8. Hoffman JM, Lucas S, Dikmen S, Braden CA, Brown AW, Brunner R, et al. Natural history of headache after traumatic brain injury. J Neurotrauma. 2011 Sep; 28(9):1719–25. https://doi.org/10.1089/neu.2011.1914 PMID: 21732765.

9. Andersson EE, Bedics BK, Falkmer T. Mild Traumatic Brain Injuries: A 10-Year Follow-Up. J Rehabil Med. 2011 Mar; 43(4):323–9. English. https://doi.org/10.2340/16501977-0666 PMID: 21271211

10. Lucas S, Hoffman JM, Bell KR, Walker W, Dikmen S. Characterization of headache after traumatic brain injury. Cephalalgia. 2012 Jun; 32(8):600–6. English. https://doi.org/10.1177/0333102412445224 PMID: 22623761

11. Walker WC, Marwitz JH, Wilk AR, Ketchum JM, Hoffman JM, Brown AW, et al. Prediction of headache severity (density and functional impact) after traumatic brain injury: A longitudinal multicenter study. Cephalalgia. 2013 Sep; 33(12):998–1008. English. https://doi.org/10.1177/0333102413482197 PMID: 23575819

12. Stacey A, Lucas S, Dikmen S, Temkin N, Bell KR, Brown A, et al. Natural History of Headache Five Years after Traumatic Brain Injury. J Neurotraum. 2017 Apr; 34(8):1558–64. English.

13. Bes A, Kunkel R, Lance JW, Nappi G, Pfaffenrath V, Rose FC, et al. The International Classification of Headache Disorders, 3rd edition (beta version). Cephalalgia. 2013 Jul; 33(9):629–808. English. https://doi.org/10.1177/0333102413485658 PMID: 23771276

14. Adams AM, Serrano D, Buse DC, Reed ML, Marske V, Fanning KM, et al. The impact of chronic migraine: The Chronic Migraine Epidemiology and Outcomes (CaMEO) Study methods and baseline

results. Cephalalgia. 2015 Jun; 35(7):563–78. English. https://doi.org/10.1177/0333102414552532 PMID: 25304766

15. Natoli JL, Manack A, Dean B, Butler Q, Turkel CC, Stovner L, et al. Global prevalence of chronic migraine: A systematic review. Cephalalgia. 2010 May; 30(5):599–609. English. https://doi.org/10.1111/j.1468-2982.2009.01941.x PMID: 19614702

16. Bogoslovsky T, Wilson D, Chen Y, Hanlon D, Gill J, Jeromin A, et al. Increases of Plasma Levels of Glial Fibrillary Acidic Protein, Tau, and Amyloid beta up to 90 Days after Traumatic Brain Injury. J Neurotraum. 2017 Jan 1; 34(1):66–73. English.

17. Mitra B, Rau TF, Surendran N, Brennan JH, Thaveenthiran P, Sorich E, et al. Plasma micro-RNA biomarkers for diagnosis and prognosis after traumatic brain injury: A pilot study. J Clin Neurosci. 2017 Apr; 38:37–42. English. https://doi.org/10.1016/j.jocn.2016.12.009 PMID: 28117263

18. Passos IC, Vasconcelos-Moreno MP, Costa LG, Kunz M, Brietzke E, Quevedo J, et al. Inflammatory markers in post-traumatic stress disorder: a systematic review, meta-analysis, and meta-regression. Lancet Psychiat. 2015 Nov; 2(11):1002–12. English.

19. Kobrosly R, van Wijngaarden E. Associations between immunologic, inflammatory, and oxidative stress markers with severity of depressive symptoms: An analysis of the 2005–2006 National Health and Nutrition Examination Survey. Neurotoxicology. 2010 Jan; 31(1):126–33. English. https://doi.org/10.1016/j.neuro.2009.10.005

20. Ramon C, Cernuda-Morollon E, Pascual J. Calcitonin gene-related peptide in peripheral blood as a biomarker for migraine. Curr Opin Neurol. 2017 Jun; 30(3):281–6. English. https://doi.org/10.1097/WCO.0000000000000440 PMID: 28234796

21. Ceylan M, Bayraktutan OF, Becel S, Atis O, Yalcin A, Kotan D. Serum levels of pentraxin-3 and other inflammatory biomarkers in migraine: Association with migraine characteristics. Cephalalgia. 2016 May; 36(6):518–25. English. https://doi.org/10.1177/0333102415598757 PMID: 26243757

22. Nordstrom A, Nordstrom P. Traumatic brain injury and the risk of dementia diagnosis: A nationwide cohort study. PLoS Med. 2018 Jan; 15(1):e1002496. https://doi.org/10.1371/journal.pmed.1002496 PMID: 29381704. Epub 2018/01/31.

23. Hocker JR, Deb SJ, Li M, Lerner MR, Lightfoot SA, Quillet AA, et al. Serum Monitoring and Phenotype Identification of Stage I Non-Small Cell Lung Cancer Patients. Cancer Invest. 2017 Oct 21; 35(9):573–85. Epub 2017/09/28. English. https://doi.org/10.1080/07357907.2017.1373120 PMID: 28949774

24. Hocker JR, Postier RG, Li M, Lerner MR, Lightfoot SA, Peyton MD, et al. Discriminating patients with early-stage pancreatic cancer or chronic pancreatitis using serum electrospray mass profiling. Cancer Lett. 2015 Apr 10; 359(2):314–24. English. https://doi.org/10.1016/j.canlet.2015.01.035 PMID: 25637792

25. Jeter CB, Hergenroeder GW, Hylin MJ, Redell JB, Moore AN, Dash PK. Biomarkers for the diagnosis and prognosis of mild traumatic brain injury/concussion. J Neurotrauma. 2013 Apr 15; 30(8):657–70. https://doi.org/10.1089/neu.2012.2439 PMID: 23062081. Epub 2012/10/16.

26. Vachani A, Pass HI, Rom WN, Midthun DE, Edell ES, Laviolette M, et al. Validation of a multiprotein plasma classifier to identify benign lung nodules. J Thorac Oncol. 2015 Apr; 10(4):629–37. https://doi.org/10.1097/JTO.0000000000000447 PMID: 25590604. Epub 2015/01/16.

27. Tuck MK, Chan DW, Chia D, Godwin AK, Grizzle WE, Krueger KE, et al. Standard Operating Procedures for Serum and Plasma Collection: Early Detection Research Network Consensus Statement Standard Operating Procedure Integration Working Group. J Proteome Res. 2009 Jan; 8(1):113–7. Epub 2008/12/17. English. https://doi.org/10.1021/pr800545q PMID: 19072545

28. Dittmar GAG, Wilkinson CRM, Jedrzejewski PT, Finley D. Role of a ubiquitin-like modification in polarized morphogenesis. Science. 2002 Mar 29; 295(5564):2442–6. English. https://doi.org/10.1126/science.1069989 PMID: 11923536

29. Ransohoff DF. Rules of evidence for cancer molecular-marker discovery and validation. Nat Rev Cancer. 2004 Apr; 4(4):309–14. https://doi.org/10.1038/nrc1322 PMID: 15057290. Epub 2004/04/02.

30. Guan W, Zhou M, Hampton CY, Benigno BB, Walker LD, Gray A, et al. Ovarian cancer detection from metabolomic liquid chromatography/mass spectrometry data by support vector machines. BMC Bioinformatics. 2009 Aug 22; 10:259. https://doi.org/10.1186/1471-2105-10-259 PMID: 19698113.

31. Baker SG, Kramer BS, Srivastava S. Markers for early detection of cancer: statistical guidelines for nested case-control studies. BMC Med Res Methodol. 2002; 2:4. https://doi.org/10.1186/1471-2288-2-4 PMID: 11914137. Epub 2002/03/27.

32. Cohen J. Statistical Power Analysis for the Behavioral-Sciences—Cohen,J. Percept Motor Skill. 1988 Dec; 67(3):1007-. English.

33. Soper DS. Post-hoc Statistical Power Calculator for a Student t-Test [Software] http://www.danielsoper.com/statcalc. 2018.

34. Altman DG, Bland JM. Diagnostic-Tests-2—Predictive Values.4. Brit Med J. 1994 Jul 9; 309 (6947):102-. English.

35. Altman DG, Bland JM. Diagnostic tests. 1: Sensitivity and specificity. BMJ. 1994 Jun 11; 308 (6943):1552. PMID: 8019315.

36. Li J, Meng HQ, Cao W, Qiu T. lMiR-335 is involved in major depression disorder and antidepressant treatment through targeting GRM4. Neurosci Lett. 2015 Oct 8; 606:167–72. English. https://doi.org/10. 1016/j.neulet.2015.08.038

37. Hek K, Mulder CL, Luijendijk HJ, van Duijn CM, Hofman A, Uitterlinden AG, et al. The PCLO gene and depressive disorders: replication in a population-based study. Hum Mol Genet. 2010 Feb 15; 19(4):731–4. English. https://doi.org/10.1093/hmg/ddp529 PMID: 19942622

38. Mbarek H, Milaneschi Y, Hottenga JJ, Ligthart L, de Geus EJC, Ehli EA, et al. Genome-Wide Signifi-cance for PCLO as a Gene for Major Depressive Disorder. Twin Res Hum Genet. 2017 Aug; 20(4):267–70. English. https://doi.org/10.1017/thg.2017.30 PMID: 28540843

39. Suidan GL, Brill A, De Meyer SF, Voorhees JR, Cifuni SM, Cabral JE, et al. Endothelial Von Willebrand Factor Promotes Blood-Brain Barrier Flexibility and Provides Protection From Hypoxia and Seizures in Mice. Arterioscl Throm Vas. 2013 Sep; 33(9):2112–20. English.

40. Kuramoto T, Kitada K, Inui T, Sasaki Y, Ito K, Hase T, et al. Attractin/mahogany/zitter plays a critical role in myelination of the central nervous system. Proc Natl Acad Sci U S A. 2001 Jan 16; 98(2):559–64. https://doi.org/10.1073/pnas.98.2.559 PMID: 11209055. Epub 2001/02/24.

41. Kozler P, Sobek O, Pokorny J. Signs of Myelin Impairment in Cerebrospinal Fluid After Osmotic Open-ing of the Blood-Brain Barrier in Rats. Physiol Res. 2015; 64:S603–S8. English. PMID: 26674284

42. Zhao YH, Li DD, Zhao JJ, Song JN, Zhao YL. The role of the low-density lipoprotein receptor-related protein 1 (LRP-1) in regulating blood-brain barrier integrity. Rev Neuroscience. 2016 Aug; 27(6):623–34. English.

43. Chasman DI, Schurks M, Anttila V, de Vries B, Schminke U, Launer LJ, et al. Genome-wide association study reveals three susceptibility loci for common migraine in the general population. Nat Genet. 2011 Jul; 43(7):695–U116. English. https://doi.org/10.1038/ng.856 PMID: 21666692

44. Liu CC, Hu J, Zhao N, Wang J, Wang N, Cirrito JR, et al. Astrocytic LRP1 Mediates Brain Abeta Clear-ance and Impacts Amyloid Deposition. J Neurosci. 2017 Apr 12; 37(15):4023–31. https://doi.org/10. 1523/JNEUROSCI.3442-16.2017

45. Shibata N, Ohnuma T, Higashi S, Higashi M, Usui C, Ohkubo T, et al. Genetic association between Notch4 polymorphisms and Alzheimer's disease in the Japanese population. J Gerontol A Biol Sci Med Sci. 2007 Apr; 62(4):350–1. PMID: 17452726.

46. Chuang TY, Guo Y, Seki SM, Rosen AM, Johanson DM, Mandell JW, et al. LRP1 expression in micro-glia is protective during CNS autoimmunity. Acta Neuropathol Commun. 2016 Jul 11; 4(1):68. https:// doi.org/10.1186/s40478-016-0343-2 PMID: 27400748. Epub 2016/07/13.

47. Starokadomskyy P, Gemelli T, Rios JJ, Xing C, Wang RC, Li H, et al. DNA polymerase-alpha regulates the activation of type I interferons through cytosolic RNA:DNA synthesis. Nat Immunol. 2016 May; 17 (5):495–504. https://doi.org/10.1038/ni.3409 Epub 2016/03/29.

48. Weiss LA, Veenstra-VanderWeele J, Newman DL, Kim SJ, Dytch H, McPeek MS, et al. Genome-wide association study identifies ITGB3 as a QTL for whole blood serotonin. Eur J Hum Genet. 2004 Nov; 12(11):949–54. English. https://doi.org/10.1038/sj.ejhg.5201239 PMID: 15292919

49. Sokolov AY, Lyubashina OA, Panteleev SS. The role of serotonin receptors in migraine headaches. Neurochem J+. 2011 Jun; 5(2):92–9. English.

50. Lee JH, Koh SQ, Guadagna S, Francis PT, Esiri MM, Chen CP, et al. Altered relaxin family receptors RXFP1 and RXFP3 in the neocortex of depressed Alzheimer's disease patients. Psychopharmacology (Berl). 2016 Feb; 233(4):591–8. https://doi.org/10.1007/s00213-015-4131-7 PMID: 26542729.

51. Seripa D, Matera MG, Franceschi M, Daniele A, Bizzarro A, Rinaldi M, et al. The RELN locus in Alzhei-mer's disease. J Alzheimers Dis. 2008 Jul; 14(3):335–44. PMID: 18599960.

52. Zhou J, Liu Q, Mao M, Tong Y. Huwe1 as a therapeutic target for neural injury. Genet Mol Res. 2014; 13 (2):4320–5. English. https://doi.org/10.4238/2014.June.9.18 PMID: 25036176

53. Barton A, Eyre S, Ke X, Hinks A, Bowes J, Flynn E, et al. Identification of AF4/FMR2 family, member 3 (AFF3) as a novel rheumatoid arthritis susceptibility locus and confirmation of two further pan-autoim-mune susceptibility genes. Hum Mol Genet. 2009 Jul 1; 18(13):2518–22. https://doi.org/10.1093/hmg/ ddp177 PMID: 19359276. Epub 2009/04/11.

54. Araki Y, Mimura T. The Histone Modification Code in the Pathogenesis of Autoimmune Diseases. Medi-ators Inflamm. 2017; 2017:2608605. https://doi.org/10.1155/2017/2608605 PMID: 28127155. Epub 2017/01/28.

55. Dickinson JD, Sweeter JM, Warren KJ, Ahmad IM, De Deken X, Zimmerman MC, et al. Autophagy regulates DUOX1 localization and superoxide production in airway epithelial cells during chronic IL-13 stimulation. Redox Biol. 2018 Apr; 14:272–84. https://doi.org/10.1016/j.redox.2017.09.013 PMID: 28982074. Epub 2017/10/06.

56. Kulikova E, Kulikov A. Striatal-enriched Tyrosine Protein Phosphatase (STEP) in the Mechanisms of Depressive Disorders. Curr Protein Pept Sc. 2017; 18(11):1152–62. English.

57. Ayoglu B, Mitsios N, Kockum I, Khademi M, Zandian A, Sjoberg R, et al. Anoctamin 2 identified as an autoimmune target in multiple sclerosis. Proc Natl Acad Sci U S A. 2016 Feb 23; 113(8):2188–93. https://doi.org/10.1073/pnas.1518553113 PMID: 26862169. Epub 2016/02/11.

58. Megiorni F, Pizzuti A. HLA-DQA1 and HLA-DQB1 in Celiac disease predisposition: practical implications of the HLA molecular typing. J Biomed Sci. 2012 Oct 11; 19:88. https://doi.org/10.1186/1423-0127-19-88 PMID: 23050549. Epub 2012/10/12.

59. Lahiri A, Hedl M, Abraham C. MTMR3 risk allele enhances innate receptor-induced signaling and cytokines by decreasing autophagy and increasing caspase-1 activation. Proc Natl Acad Sci U S A. 2015 Aug 18; 112(33):10461–6. https://doi.org/10.1073/pnas.1501752112 PMID: 26240347. Epub 2015/08/05.

60. Tian Y, Chang JC, Fan EY, Flajolet M, Greengard P. Adaptor complex AP2/PICALM, through interaction with LC3, targets Alzheimer's APP-CTF for terminal degradation via autophagy. Proc Natl Acad Sci U S A. 2013 Oct 15; 110(42):17071–6. https://doi.org/10.1073/pnas.1315110110 PMID: 24067654. Epub 2013/09/27.

61. Schurks M. Genetics of migraine in the age of genome-wide association studies. J Headache Pain. 2012 Jan; 13(1):1–9. English. https://doi.org/10.1007/s10194-011-0399-0 PMID: 22072275

62. Maher BH, Taylor M, Stuart S, Okolicsanyi RK, Roy B, Sutherland HG, et al. Analysis of 3 common polymorphisms in the KCNK18 gene in an Australian Migraine Case-control cohort. Gene. 2013 Oct 10; 528(2):343–6. English. https://doi.org/10.1016/j.gene.2013.07.030 PMID: 23911303

63. Rubino E, Fenoglio P, Gallone S, Govone F, Vacca A, De Martino P, et al. Genetic variants in the NOTCH4 gene influence the clinical features of migraine. J Headache Pain. 2013;14. English.

64. Ogawa M, Yoshikawa Y, Kobayashi T, Mimuro H, Fukumatsu M, Kiga K, et al. A Tecpr1-dependent selective autophagy pathway targets bacterial pathogens. Cell Host Microbe. 2011 May 19; 9(5):376–89. https://doi.org/10.1016/j.chom.2011.04.010 PMID: 21575909. Epub 2011/05/18.

65. Kim TS, Kawaguchi M, Suzuki M, Jung CG, Asai K, Shibamoto Y, et al. The ZFHX3 (ATBF1) transcription factor induces PDGFRB, which activates ATM in the cytoplasm to protect cerebellar neurons from oxidative stress. Dis Model Mech. 2010 Nov-Dec; 3(11–12):752–62. English. https://doi.org/10.1242/dmm.004689 PMID: 20876357

66. Villanueva J, Shaffer DR, Philip J, Chaparro CA, Erdjument-Bromage H, Olshen AB, et al. Differential exoprotease activities confer tumor-specific serum peptidome patterns. J Clin Invest. 2006 Jan; 116 (1):271–84. English. https://doi.org/10.1172/JCI26022 PMID: 16395409

67. Bianchi ME. DAMPs, PAMPs and alarmins: all we need to know about danger. J Leukocyte Biol. 2007 Jan; 81(1):1–5. English.

68. Sahyouni R, Gutierrez P, Gold E, Robertson RT, Cummings BJ. Effects of concussion on the blood–brain barrier in humans and rodents. Journal of Concussion. 2017; 1:2059700216684518. https://doi.org/10.1177/2059700216684518

69. Song H, Fang F, Tomasson G, Arnberg FK, Mataix-Cols D, Fernandez de la Cruz L, et al. Association of Stress-Related Disorders With Subsequent Autoimmune Disease. JAMA. 2018 Jun 19; 319 (23):2388–400. https://doi.org/10.1001/jama.2018.7028 PMID: 29922828. Epub 2018/06/21.

70. Li QL C.; and Tao L. Molecular mechanisms of autophagy after traumatic brain injury. Journal Histology and Histopathology Research. 2018; 1(1):2. Epub 10/15/2017.

71. Wu DJ, Adamopoulos IE. Autophagy and autoimmunity. Clin Immunol. 2017 Mar; 176:55–62. https://doi.org/10.1016/j.clim.2017.01.007 PMID: 28095319. Epub 2017/01/18.